Microelectronics Reliability 102 (2019) 113409

Contents lists available at ScienceDirect

Microelectronics Reliability

journal homepage: www.elsevier.com/locate/microrel

Analysis of Schottky emission electric charge transport mechanism in Cu-Lu_2O_3-Cu MIM structure by temperature dependent current-voltage characteristics

Shahnaz Akbar[a], Jolly Jacob[b], Khalid Mahmood[c,*], M.F. Wasiq[d], Ghulam Hassnain Jaffari[d], Muhammad Azhar Khan[e]

[a] Department of Physics, Bahauddin Zakariya University, Multan 60800, Pakistan
[b] College of Arts and Science, Abu Dhabi University, Abu Dhabi, United Arab Emirates
[c] Department of Physics, Government College University Faisalabad, 38100, Pakistan
[d] Department of Physics, Qauid-e-Azam University Islamabad, Pakistan
[e] Department of Physics, The Islamia University of Bahawalpur, Bahawalpur, 63100, Pakistan

ARTICLE INFO

Keywords:
Cu-Lu_2O_3-Cu diode
e-Beam evaporation
I-V measurements
Schottky emission
Dielectric constant

ABSTRACT

In this study, the Cu-Lu_2O_3-Cu metal-insulator-metal (MIM) structure was fabricated by electron beam evaporation method on the glass substrate with symmetric electrode configuration. The dominant conduction mechanism in fabricated MIM diode was analyzed using temperature dependent current-voltage (I-V) characteristics in temperature range 323–403 K. Schottky emission, Fowler-Nordheim (F-N) and Poole-Frankel (P-F) conduction mechanisms were tested by analyzing the I-V data according to these theories. P-F emission and Schottky emission conduction mechanisms were found to be dominant conduction mechanisms in low and high applied electric field range respectively. The Schottky emission mechanism was further studied in detail by plotting the Ln(I/T^2) Vs $V^{1/2}$ and Ln(I/T^2) Vs 1000/T plots at different applied fields and temperatures respectively. The dielectric constants were extracted from the conduction plots at various temperatures and were found to be close agreement with experimental dielectric constant of Lu_2O_3 (11). The metal-insulator barrier height and trap energy were also calculated at various measurement temperatures and discussed according to Schottky emission theory.

1. Introduction

Metal-Insulator-Metal (MIM) device can be formed by sandwiching a dielectric material between two metal electrodes [1]. These devices gaining substantial interest among the research community because of their amazing properties which make this material a potential candidate for many commercialized applications [2,3]. The other applications of MIM structures can be found in the memory devices. The principal parameter that decides the potential utilization of these structures in memory devices is the properties of dielectric material along with the type of metal electrode and thickness of dielectric material. The dielectric materials with high dielectric constant are preferred. Various materials have been used as dielectric material in the literature for example SiO_2, Al_2O_3, ZnO, HfO_2, Gd_2O_3 [4–8]. Lu_2O_3 is also entering into this family because of its unique properties, i.e. wide band gap high dielectric constant and refractive index having values 5.3–5.5 eV, 11–13 and 1.84 respectively [9–17]. But to utilized Lu_2O_3 based MIM diodes in commercial applications, it is very important to understand the charge transport mechanism across the metal-Lu_2O_3-metal device. Due to fundamental importance many researchers have attempted to understand the charge transport mechanism in such structures. For example Lee et al. investigated the charge transport mechanism in metal-SiO_2-metal and they found that space charge conduction mechanism is operative in underlying structure [18]. The choice of suitable metal is also very important because this can play vital role in controlling the type of the conduction mechanism across the metal-insulator interface. Recently our group published two research papers on the investigation of the conduction mechanism in Lu_2O_3 based MIM structures using Al and Cr metals [19,20]. Furthermore, Marnadu et al. also reported the influence of metal work function on the charge transport in metal-WO_3-metal MIM structre [21]. But we have not found any report about the investigation of the conduction

* Corresponding author.
E-mail address: Khalid_mahmood856@yahoo.com (K. Mahmood).

https://doi.org/10.1016/j.microrel.2019.113409
Received 27 December 2018; Received in revised form 23 June 2019; Accepted 4 July 2019

mechanism in Cu-Lu_2O_3-Cu MIM structure in the literature. Therefore, it is essential to probe into the charge transport behavior of the Cu-Lu2O3-Cu MIM structure to fully understand the device properties.

This research is about the investigation of the dominant charge mechanism in Cu-Lu_2O_3-Cu MIM diodes grown by electron beam evaporation method. The current-voltage (I-V) measurements were performed at various temperatures varying from 323 to 403 K to identify the underlying charge transport mechanism. The I-V data was evaluated according to F-N tunneling, P-F emission and Schottky emission theories and it was found that data was fitted well with the Schottky emission theory in high field range and P-F in low field range. Therefore, we concluded that Schottky emission charge transport is a dominant conduction mechanism in the Cu-Lu_2O_3-Cu MIM structure at high applied electric field.

2. Experimental detail

The Cu-Lu_2O_3-Cu MIM structure was fabricated on glass substrate using electron beam evaporation system (Edward EA306A England). The cleaning of substrate was performed using acetone and ethanol and substrate was loaded into e-beam chamber. The Cu metal was evaporated to grow 30 nm thick bottom electrode. After bottom electrode fabrication, 80 nm thick film of Lu_2O_3 was grown on Cu deposited glass substrate. The vacuum of 6×10^{-5} Torr was achieved in the e-beam chamber using rotary and diffusion pumps. For the growth of Lu_2O_3 thin film, we have used followings growth parameters; applied bias voltage 5.5 kV, e-beam current 110 mA and deposition rate was 0.168 nm s$^-$1. After deposition of dielectric, top Cu metal electrode was fabricated using e-beam system and the thickness of top electrode was 10 nm.

X-ray Diffraction (Bruker) was used to test the structure of grown Lu_2O_3 thin film. The current-Voltage measurements were performed in the temperature range 323–403 K in the voltage range 0–10 V is used Keithley source meter 2400 (Fig. 1).

3. Results and discussion

The room temperature I-V data of Cu-Lu_2O_3-Cu MIM diode is represented in fig. The very small amount of leakage current at 1 V suggested the typical behavior of the metal - dielectric interface. It is also evident from this graph that current is increased very slowly up to applied voltage 1 V but it increases linearly with voltage for high applied field. This type of behavior gives a clue that at least two dominance conduction mechanism are operative for complete range of applied electric field, i.e. one type of mechanism is dominant below applied field 1 V and other mechanism is dominant in high field range [22]. Therefore, to explore the dominant transport mechanisms for entire applied field, we need to redraw the I-V data according to various conduction theories such as F-N tunneling, P-F emission theory and Schottky emission theory.

The possibility of a P-F conduction mechanism can be tested by rewriting the current equation can according to the P-F emission theory as below [23].

$$J_{PF} = q\mu N_C \exp\left[\frac{-q(\phi_T - \sqrt{qE/\pi\varepsilon})}{kT}\right] \tag{1}$$

All quantities have the usual meaning. Therefore a metal-insulator-metal structure having dominant P-F conduction, Ln (I/V) versus $V^{1/2}$ graph should have a straight line. We have plotted this graph to check the possibility of P-F conduction mechanism and shown in Fig. 2. The graph in Fig. 2 clearly demonstrated that data has a linear relationship between Ln (I/V) versus $V^{1/2}$ below the applied field of 1 V but deviate from linearity above 1 V. This behavior suggested that the P-F conduction mechanism is a dominant operating mechanism in the low field range, but it may not operate in the high field region. Furthermore, we have also tested the possibility of a F-N tunneling mechanism by plotting the graph between Ln (I/V) versus 1/V (not shown here) which showed nonlinear behavior, again confirmed that F-N is also not a dominant conduction mechanism.

In order to investigate the conduction mechanism in high field range, we have tested the Schottky emission theory in high field (above 1 V). As the Schottky emission theory is depends upon both temperature

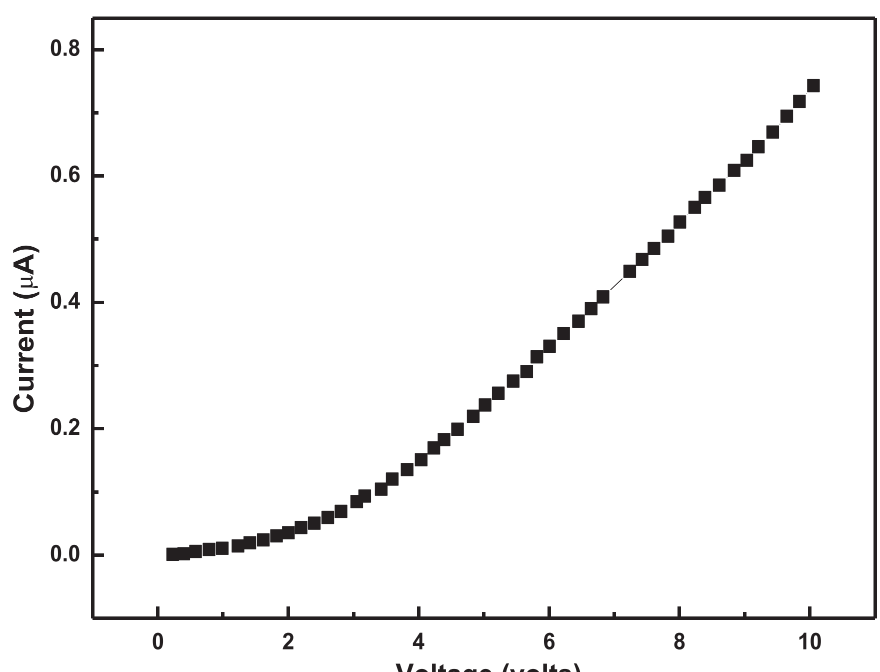

Fig. 1. Room temperature, current-voltage characteristic of Cu-Lu_2O_3-Cu metal-insulator-metal (MIM) structure. The graphs demonstrated that there are at least conduction regions.

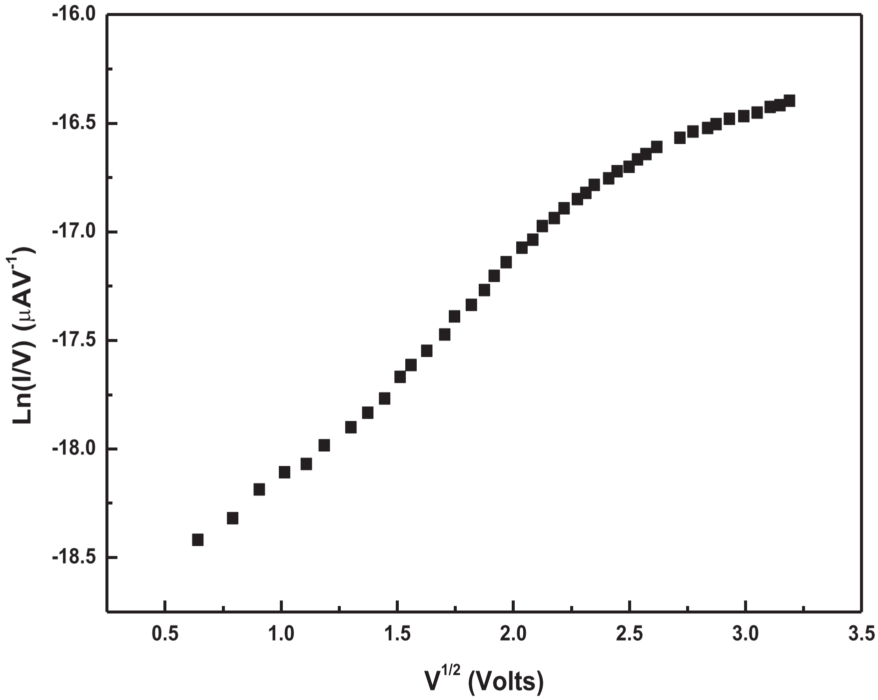

Fig. 2. The graph between Ln (I/V) versus $V^{1/2}$ for Cu-Lu_2O_3-Cu MIM structure. A straight line in the low field region suggested the presence of a P-F emission mechanism in a low field range.

and field, therefore field dependent and temperature dependent graphs are helpful to demonstrate the transport mechanism. In order to analyze the Cu-Lu_2O_3-Cu MIM structure according to the Schottky emission theory, we have rewritten the current equation as below [24].

$$I = AA_1T^2\left[\exp\left(\frac{-\Phi_0}{\mathrm{k_B T}}\right)\cdot\exp\left(\frac{\beta_S V^{1/2}}{\mathrm{k_B T d^{1/2}}}\right)\right] \tag{2}$$

Fig. 3 evident the graph between LnI versus $V^{1/2}$ for Cu-Lu_2O_3-Cu MIM structures at various temperature ranges from 323 to 403 K. The linear relationship of this graph in the high field range suggested the dominance of Schottky emission transport phenomena in fabricated MIM diodes. We have calculated the temperature dependent values of dielectric constants and are found to be increased from 7.9 to 10.7 as the temperature increased from 323 to 403 K respectively. The calculated values of dielectric constants are found to match with the reported value of dielectric constant of Lu_2O_3 which is 11 [25,26]. The close agreement of dielectric constant suggested that the Schottky emission conduction mechanism is the dominant conduction mechanism in Cu-Lu_2O_3-Cu MIM structure at high electric fields. Furthermore, this graph

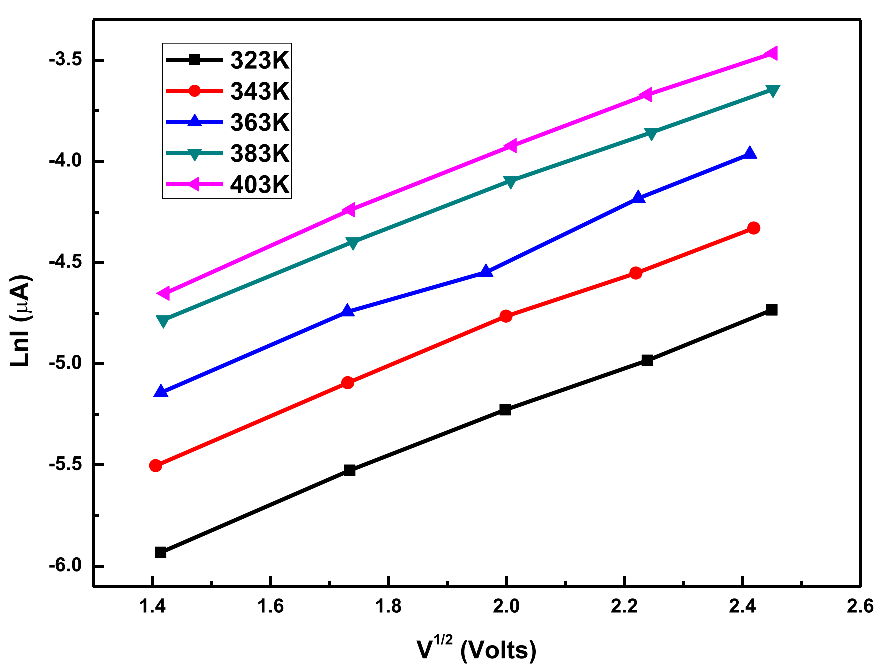

Fig. 3. The graph between $V^{1/2}$ versus LnI for MIM structure at various measurement temperatures in the temperature range 303–403 K. The straight line suggested that Schottky emission is the dominant conduction mechanism.

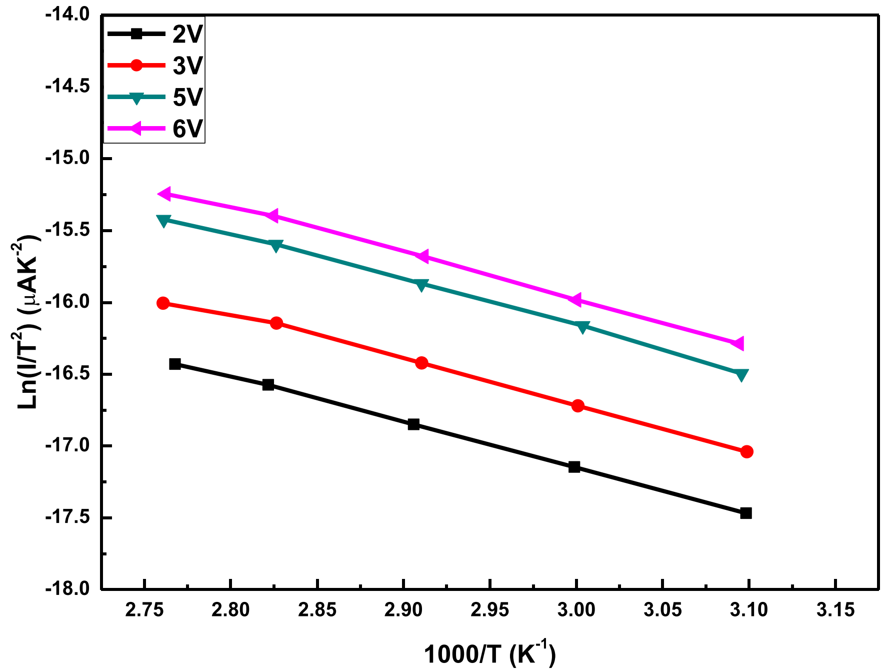

Fig. 4. Arrhenius plot of leakage current as a function of 1000/T of Cu-Lu_2O_3-Cu MIM structure at various fields ranging from 1 to 6 V.

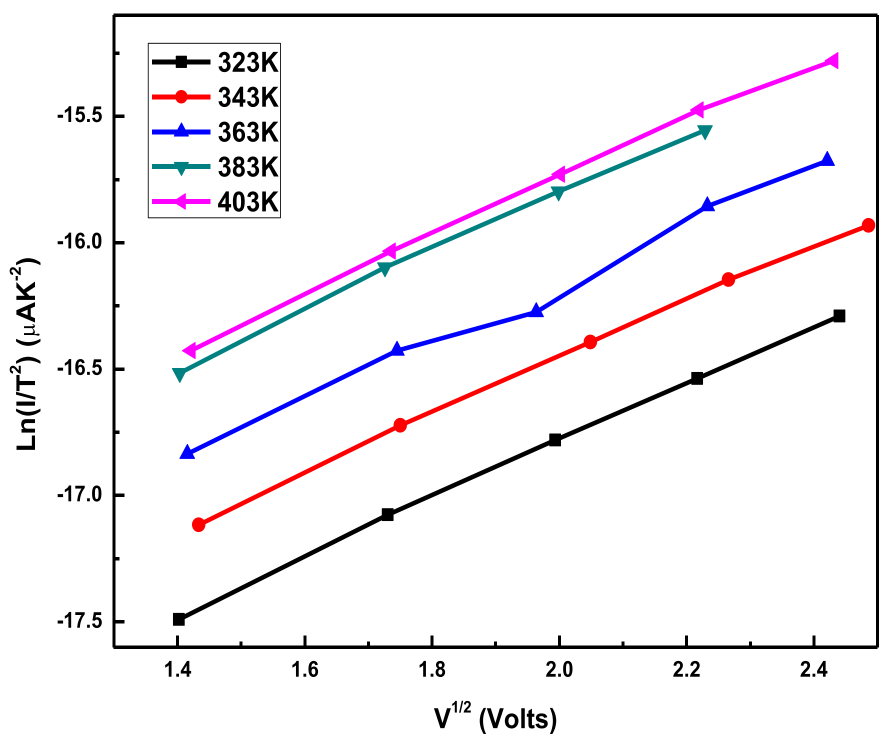

Fig. 5. The Schottky plot in the temperature range 323–403 K for Cu-Lu_2O_3-Cu for high electric field range. The linear behavior favored that Schottky emission is the dominant conduction mechanism.

also demonstrated that the density of leakage current increases with the temperature, favored the dominance of Schottky emission conduction mechanism. Our argument that charge transport across MIM structure is follow the Schottky emission theory can be further strengthened by plotting the Arrhenius and Schottky plots at various fields and temperatures respectively.

Fig. 4 demonstrated the graph of Ln (I/T^2) versus 1000/T for Cu-Lu_2O_3-Cu MIM structure at various applied fields from 1 to 6 V. The linear relationship of this graph verified again that Schottky emission conduction mechanism is operating at high applied electric field. It is also shown that the density of leakage current is also field dependent which confirmed the basic requirement that currently depends on temperature and applied field for Schottky emission mechanism.

To strengthen our argument that charge transport follows the Schottky emission theory, we have also drawn the graph between Ln (I/T^2) versus $V^{1/2}$ (Schottky plot) for Cu-Lu_2O_3-Cu MIM structure at various temperature ranges from 303 to 403 K and shown in Fig. 5. The straight line of between Ln (I/T^2) and $V^{1/2}$ also favored our argument

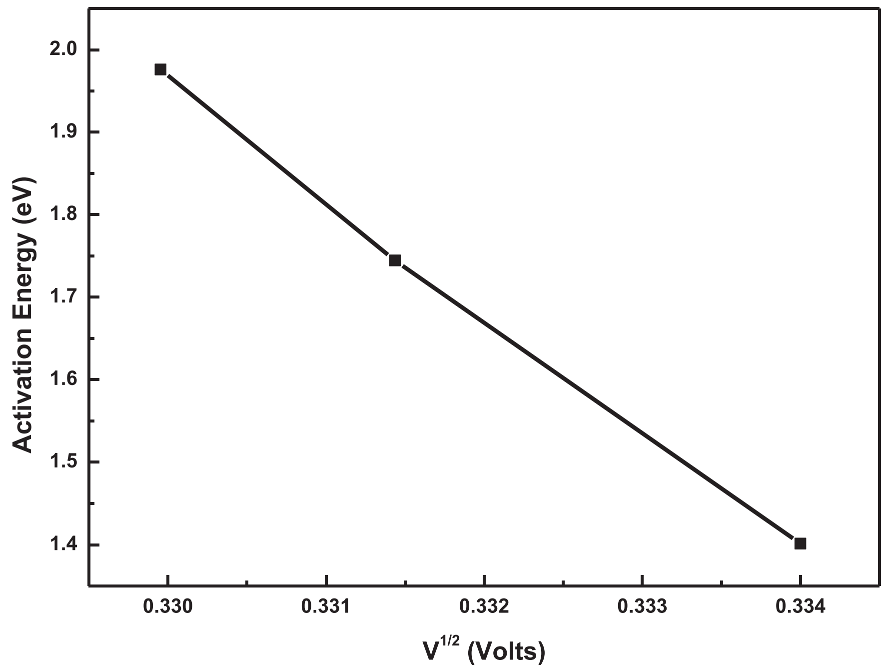

Fig. 6. Effect of $V^{1/2}$ on the activation energy of traps in dielectric material.

that movement of charge carriers across the fabricated metal-insulator-metal device obeys the laws of the Schottky emission theory at high applied electric field. It is also observed that conduction becomes stronger with increasing the measurement temperature from 323 to 403 K because the carriers gain enough thermal energy at high temperature and overcome the barrier at the metal - insulator interface. The barrier height is also calculated using the intercept of Schottky plot and room temperature value for barrier height was found to be 0.6 eV.

Fig. 6 depicts the graph between trap energy and applied electric field. The data suggested that trap activation energy decreases from 2 to 1.4 eV as the value of $V^{1/2}$ increases from 0.330 to 0.334 respectively.

4. Conclusion

In this manuscript we have fabricated a Cu-Lu_2O_3-Cu metal-insulator-metal structure using the electron beam evaporation method. The carrier conduction mechanism in the grown MIM structure was investigated by current-voltage characteristics measured in the temperature range 323–403 K. Various I-V graphs such as applied field dependent Arrhenius plot and temperature dependent Schottky plot were plotted to demonstrate the operative charge transport in the investigated structures. The data suggested that there are two conduction mechanism are operative i.e. in the low field region, P-F conduction mechanism id dominant and in the high field region, the Schottky emission conduction mechanism is dominant.

References

[1] J. Lee, K. Yoon, K.H. Lim, J.W. Park, D. Lee, N.K. Cho, Y.S. Kim, Vertical transport control of electrical charge carriers in insulator/oxide semiconductor hetero-structure, Sci. Report. 8 (2018) 5643.

[2] J.J. Huang, C.W. Kuo, W.C. Chang, T.H. Hou, Transition of stable rectification to resistive-switching in Ti/TiO_2/Pt oxide diode, Appl. Phys. Lett. 96 (2010) 262901.

[3] J. Hou, S.S. Nonnenmann, W. Qin, D.A. Bonnell, Size dependence of resistive switching at nanoscale metal-oxide interfaces, Adv. Funct. Mater. 24 (2014) 4113–4118.

[4] A.D. Weerakkody, N. Sedghi, I.Z. Mitrovic, H. Van Zalinge, I. Nemr Noureddine, S. Hall, J.S. Wrench, P.R. Chalker, L.J. Phillips, R. Treharne, K. Durose, Enhanced low voltage non-linearity in resonant tunneling metal-insulator-insulator-metal structure, Microelectron. Eng. 147 (2015) 298.

[5] P. Jancovi, B. Hude, E. Dobrock, J. Dérer, J. Fedor, K. Fröhlich, Resistive switching HfO_2 based atomic layer deposition grown metal-insulator-metal structures, App. Surf. Sci. 312 (2014) 112.

[6] S. Mansouri, L.E. Mir, A.A. Al-Ghamdi, F. El-Tantawy, F. Yakuphanoglu, Modeling of current–voltage and capacitance–voltage characteristics of pentacene and sol–gel derived SiO2 gate dielectric layer based on thin-film transistor, Syn. Meter. 199 (2015) 159.

[7] S. Krishnan, E. Stefanakos, S. Bhansali, Effects of dielectric thickness and contact area on current–voltage characteristics of thin film metal–insulator–metal diodes, Thin Solid Films 516 (2008) 2244–2250.

[8] M.F. Wasiq, K. Mahmood, F. Aen, F.M. Warsi, M.A. Khan, Investigation of high temperature charge transport mechanism in Al-Gd_2O_3-Al based metal-insulator-metal structures, Appl. Phys. A Mater. Sci. Process. 122 (2016) 1046.

[9] S.V. Ordin, A.I. Shelykh, Semiconductors 44 (2010) 558.

[10] V.V. Afanas'ev, S. Shamuilia, M. Badylevich, A. Stesmans, L.F. Edge, W. Tian, D.G. Schlom, J.M.J. Lopez, M. Roeckerath, J. Schubert, Electronic structure of silicon interfaces with amorphous and epitaxial insulating oxides: Sc2O3, Lu2O3, LaLuO3, Microelectron. Eng. 84 (2007) 2278.

[11] M. Guzik, J. Pejchal, A. Yoshikawa, A. Ito, T. Goto, M. Siczek, T. Lis, G. Boulon, Structural investigations of Lu2O3 as single crystal and polycrystalline transparent ceramic, Crys. Grow. Design. 14 (2014) 3327.

[12] G. Scarel, E. Bonera, C. Wiemer, G. Tallarida, S. Spiga, M. Fanciulli, I.L. Fedushkin, H. Schumann, Atomic layer deposition of Lu_2O_3, Appl. Phys. Lett. 85 (2004) 630.

[13] C. Li, F. Zhang, Y. Wu, X. Zhang, Influence of strain rate effect on material removal and deformation mechanism based on ductile nanoscratch tests of Lu2O3 single crystal, Cerm. Inter. 44 (2018) 21486.

[14] G. Adaschi, N. Imanaga, The binary rare earth oxides, Chem. Rev. 98 (1998) 1479.

[15] L. An, A. Ito, T. Goto, Effects of ball milling and post-annealing on the transparency of spark plasma sintered Lu2O3, Ceram. Int. 37 (2011) 2263.

[16] A. Pavlik III, S.V. Ushakov, A. Navrotsky, C.J. Benmore, Structure and thermal expansion of Lu_2O_3 and Yb_2O_3 up to the melting points, J. Nucl. Mater. 495 (2017) 385.

[17] S. Ohmi, M. Takeda, H. Ishiwara, H. Iwai, Electrical characteristics for Lu_2O_3 thin films fabricated by e-beam deposition method, J. Electrochem. Soc. 151 (2004) G279.

[18] J. Lee, K.-H.L. KapsooYoon, J.-W. Park, D. Lee, N.-K. Cho, Y.S. Kim, Vertical transport control of electrical charge carriers in insulator/oxide semiconductor hetero-structure, Sci. Rep. 8 (2018) 5643.

[19] S. Akbar, K. Mahmood, M.F. Wasiq, M.Y. Nadeem, M.A. Khan, Field and temperature dependent current-voltage characteristics of Al-Lu_2O_3-Al metal-insulator-metal diodes, Phys. B 520 (2017) 112.

[20] K. Mahmood, S. Akbar, M. Ramzan, M.F. Wasiq, M.A. Khan, Growth and electrical characterization of Cr-Lu_2O_3-Cr MIM structure by electron beam evaporation technique, Matter. Res. Exp. 6 (2019) 010605.

[21] R. Marnadu, J. Chandrasekaran, M. Raja, M. Balaji, S. Maruthamuthu, P. Balraju, Influence of metal work function and incorporation of Sr atom on WO3 thin films for MIS and MIM structured SBDs, Supperlattices and microstructures 119 (2018) 134.

[22] S. Grover, G. Moddel, Engineering the current–voltage characteristics of metal–insulator–metal diodes using double-insulator tunnel barriers, Solid State Electron 67 (2012) 94–99.

[23] F. C. Chiu, A review on conduction mechanism in dielectric films, Adv. Mater. Sci. Eng. 578168 (2014) 1–18.

[24] H.-Y. Kwak, H.-M. Kwon, Y.-J. Jung, S.-K. Kwon, J.-H. Jang, W.-I. Choi, M.-L. Ha, J.-I. Lee, H.-D. Lee, Solid State Electron. 79 (2013) 218.

[25] F.C. Chiu, C.M. Lai, Optical and electrical characterizations of cerium oxide thin films, J. Phys. D 43 (2010) 1–5.

[26] T. Wiktorczyk, Mater. Sci.-Pol. 27 (2009) 1179.